# Accurate second-order susceptibility measurements of visible and infrared nonlinear crystals

Michael M. Choy* and Robert L. Byer
*Applied Physics Department, Microwave Laboratory, W. W. Hansen Laboratories of Physics, Stanford University, Stanford, California*
(Received 8 December 1975)

Using the wedge technique we have directly compared the second-order nonlinear susceptibilities of infrared and visible nonlinear crystals. The measured nonlinear coefficient ratios at 2.12 $\mu$m relative to $d_{31}(LiIO_3)$ are: for $LiNbO_3$ ($d_{33}$), $4.53 \pm 4.3$; GaP ($d_{36}$), $12.1 \pm 1.7$; GaAs ($d_{36}$), $26.9 \pm 2.1$; $AgGaSe_2$ ($d_{36}$), $10.5 \pm 1.2$; CdSe ($d_{33}$), $10.2 \pm 1.2$. The measured ratios at 1.318 $\mu$m relative to $d_{31}(LiIO_3)$ are: for $LiIO_3$ ($d_{33}$), $0.990 \pm 0.05$; $LiNbO_3$ ($d_{31}$), $0.870 \pm 0.07$; $LiNbO_3$ ($d_{33}$), $4.66 \pm 0.56$; $KH_2PO_4$ ($d_{36}$), $0.088 \pm 0.01$; GaP ($d_{36}$), $12.0 \pm 1.2$. We have used the parametric fluorescence method to accurately measure the absolute second-order susceptibility of $LiIO_3$ ($d_{31}$) and $LiNbO_3$ ($d_{31}$) at 4880 and 5145 Å. Our recommended values for $d_{31}(LiIO_3) = (7.31 \pm 0.62) \times 10^{-12}$ and $d_{31}(LiNbO_3) = (5.82 \pm 0.70) \times 10^{-12}$ m/V agree very well with previous independent absolute measurements. By scaling the nonlinear susceptibilities through the relatively dispersionless Miller's $\Delta$ and using the wedge ratio results, we have, for the first time, established a uniform scale of nonlinear susceptibility values relative to $d_{31}(LiIO_3)$ that extends from 0.488 to 10.6 $\mu$m in the infrared.

## I. INTRODUCTION

The absolute magnitude of the second-order nonlinear susceptibilities is important in determining the conversion efficiency and threshold of nonlinear devices such as harmonic generators, up-converters, mixers, and parametric oscillators. Accurate values of second-order susceptibilities are also of interest for theoretical considerations for the understanding of the origin of the nonlinear optical susceptibilities. This understanding is important in material assessment and the prediction of new material characteristics of interest in improved nonlinear optical devices.

The difficulty of measuring absolute susceptibility values has led to the practice of making relative measurements against "known" standard crystals. In the visible spectral region, $SiO_2$, $KH_2PO_4$ (KDP), $NH_4H_2PO_4$(ADP),[1] and recently $LiIO_3$,[2] have been used as reference standards. In the infrared, GaAs (Ref. 3) and GaP (Ref. 4) have become reference crystals. Unfortunately, the limited transparency range overlap of visible and infrared transmitting crystals has prevented a direct comparison of the infrared and visible nonlinear susceptibilities. Using the wedge technique we have accurately compared the nonlinear susceptibilities of GaAs, GaP, CdSe, $AgGaSe_2$, $LiNbO_3$, $LiIO_3$, and KDP.

Of equal importance, we have accurately redetermined the absolute nonlinear susceptibility of $LiIO_3$ and $LiNbO_3$ by the parametric fluorescence method. We therefore, have established an absolute nonlinear susceptibility scale that extends over the visible and infrared wavelength range.

In Sec. II we describe the absolute susceptibility measurements by the parametric fluorescence method. The $LiIO_3$ and $LiNbO_3$ measured susceptibilities at 4880 Å are in close agreement with previous parametric fluorescence results. In Sec. III we describe the relative susceptibility measurements using the wedge technique at 2.12 and 1.318 $\mu$m wavelengths. Wavelength scaling of the measured susceptibilities through Miller's $\Delta$ is also discussed. Finally, in Sec. IV we compare and discuss our results with previous measurements and we recommend a set of values of nonlinear susceptibilities at various visible and infrared wavelengths.

## II. ABSOLUTE SUSCEPTIBILITY MEASUREMENTS OF $LiIO_3$ AND $LiNbO_3$

Absolute nonlinear susceptibilities can be measured by second-harmonic generation[5,6] optical rectification,[7] sum and difference frequency[8] generation. In all of the above methods an absolute power must be measured to determine the nonlinear coefficient. Furthermore, the generated signal is dependent on the laser spatial and axial mode conditions[9] and upon focusing of the pump beam into the nonlinear crystal.[10] The combination of these factors has limited the measurement accuracy of the second-order susceptibility by the above methods.

The second-order susceptibility can also be determined by Raman scattering[11,12] and by parametric fluorescence.[13,14] These methods require only that a power ratio be measured instead of an absolute power and they are not dependent upon laser mode behavior or upon focusing.[11] Of the two methods only parametric fluorescence pro-

vides a direct measurement of the nonlinear susceptibility.

### A. Parametric fluorescence theory

Parametric fluorescence was first observed by Harris *et al.* in $LiNbO_3$.[15] The method was soon extended to[16] ADP and recently to other materials.[14,16] Byer and Harris[13] developed a semiclassical theoretical description of parametric fluorescence and used the method to measure the absolute susceptibility of $LiNbO_3$. Parametric fluorescence has also been theoretically treated by Giallorenzi and Tang[17] and by Kleinman.[18] Giallorenzi and Tang used a scattering theory approach and Kleinman applied the golden rule to describe the process. Byer[19] has shown the equivalence of the three theoretical treatments.

Following Byer and Harris[13] we write for the power scattered from the incident pump beam into the signal beam integrated over the small angle $\varphi$ about the pump beam direction and over the frequency interval $d\omega_s$:

$$P_S = \beta l^2 P_p \int_{-\infty}^{\infty} \int_0^{\theta} [\mathrm{sinc}^2(\tfrac{1}{2}\Delta kl)]\varphi \, d\varphi \, d\omega_s .$$

where $\mathrm{sinc}(\frac{1}{2}\Delta kl)$ denotes $(2/\Delta kl)\sin(\frac{1}{2}\Delta kl)$. Here $\omega_p = \omega_s + \omega_i$ and in the small-angle approximation

$$\Delta k = k_p - k_s - k_i + (k_s k_p / k_i)\tfrac{1}{2}\varphi^2$$

or

$$\Delta k = -b d\omega_s + g\varphi^2 ,$$

with

$$b = \left(\frac{\partial k_s}{\partial \omega_s} - \frac{\partial k_i}{\partial \omega_i}\right) = \frac{1}{c}\left[n_s - n_i - \lambda_s\left(\frac{dn_s}{d\lambda_s}\right) + \lambda_i\left(\frac{dn_i}{d\lambda_i}\right)\right]$$

and

$$g = k_s k_p / 2k_i ,$$

where $c$ is the velocity of light and $n$ is the refractive index of the nonlinear crystal.

Integrating over angle and frequency we find for the total parametric fluorescence power at the signal frequency

$$P_s = (\beta l P_p / b)\pi\theta^2 , \tag{1}$$

where $\theta$ is the acceptance angle within the nonlinear crystal, $l$ is the crystal length, and

$$\beta = 2\omega_s^4 \omega_i d_{\mathrm{eff}}^2 \hbar n_s / (2\pi)^2 \epsilon_0 c^5 n_i n_p . \tag{2}$$

Here $d_{\mathrm{eff}}$ is the effective nonlinear coefficient[10] which for 90° phase matched $LiNbO_3$ is $d_{31}$ and for angle phase matched $LiIO_3$ is $d_{31}\sin(\theta+\rho)$ where $\rho$ is the double refraction angle. The result shows that the signal power varies linearly with pump power and thus is independent of the pump mode structure and of focusing.

The measurement procedure is therefore to accurately measure the power ratio $P_s/P_p$ at a fixed frequency, crystal length, and acceptance angle. Using known crystal indices of refraction to determine the dispersion factor $b$ then yields the nonlinear coefficient

$$d_{\mathrm{eff}} = [P_s b \epsilon_0 \lambda_s^4 \lambda_i n_i n_p / P_p \theta^2 l 2(2\pi)^3 \hbar n_s]^{1/2} . \tag{3}$$

### B. Absolute susceptibility measurements

The experimental arrangement is shown schematically in Fig. 1. An argon-ion laser operating at 4880 and 5145 Å was used as a pump source. The laser beam was polarized and then sent through a chopper and spike filter before reaching the sample. Since all laboratory surfaces fluoresce, care was taken to see that a minimum of surfaces were encountered prior to the crystal. The crystal was followed by an analyzer, a long pass filter to eliminate the residual pump beam, a lens and aperture arrangement for defining the acceptance angle $\theta$,[13] and a cooled RCA 7265 photomultiplier tube preceeded by a 6328-Å spike filter. The signal was detected using a PAR HR-8 lock-in amplifier. A separate HeNe laser was used to calibrate the photomultiplier and the required neutral density filters.

The measurement procedure consisted of calibrating the neutral density filters at 6328 Å using the phase-sensitive amplifier. A total of 80 dB of attenuation was required to reduce the 5-mW HeNe beam to the level of the parametric fluorescence. The crystal was then carefully aligned and tuned to generate parametric fluorescence peaked at 6328 Å. For the case of $LiIO_3$ two crystal cuts were used, one at 28.7° and the other at 24.1° for the 4880- and 5145-Å pump wavelengths. As a cross check a measurement was made with the 24.1° sample at 4880 Å. The $LiIO_3$ crystal samples

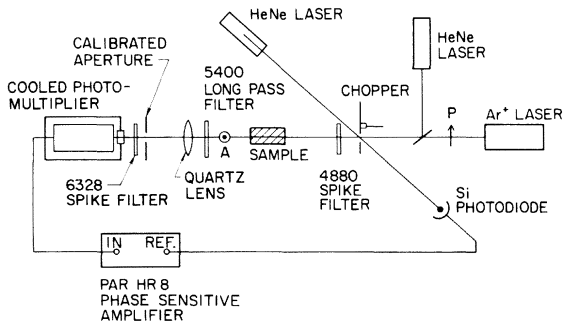


EXPERIMENTAL SCHEMATIC FOR PARAMETRIC FLUORESCENCE

FIG. 1. Experimental schematic for parametric fluorescence measurements of $d_{31}(LiIO_3)$ and $d_{31}(LiNbO_3)$.

TABLE I. Absolute susceptibilities of $LiIO_3$ and $LiNbO_3$ by parametric fluorescence. Numbers in ( ) indicate independent measurments at different solid angle apertures.

| Material | $\lambda_p$ (Å) | Crystal cut | $\theta_m$ (meas.) | $\theta_m$ (calc.) | $d_{31}$ (meas.) ($10^{-12}$ m/V) | Weighted average $d_{31}$ ($10^{-12}$ m/V) |
|---|---|---|---|---|---|---|
| $LiIO_3$ | 4880 | 28.7° | 28.1° | 28.05 | 7.31(3) | 7.215 |
| | | | 27.8° | | 7.23(4) | |
| | | 24.1° | 27.55° | | 7.10(3) | |
| | 5145 | 24.1° | 24.1° | 24.9° | 7.43(3) | 7.33 |
| | | | 24.1° | | 7.23(3) | |
| $LiNbO_3$ | 4880 | 90° − $a$ | $T_m$ = 165 °C | | 5.88(3) | 5.823 |
| | | 90° − $b$ [a] | | | 5.78(4) | |

[a] Sample in an oxygen atmosphere.

were 1×1 $cm^2$ by 2.00 cm long with an antireflection coated high-quality optical surface. $LiNbO_3$ was 90° phasematched by adjusting the crystal temperatures to 165 °C with the aid of a Chromatix oven. The $LiNbO_3$ crystal was 5 mm×5 mm ×1.70 cm long and was prepared from a congruently grown boule.

The measurement procedure consisted of determining the argon-ion laser pump power with an Eppley Thermopile after attenuation from approximately 100 to 10 mW by a calibrated neutral density filter. The HeNe power was also measured with the Eppley Thermopile. The neutral density filters were then inserted into the HeNe beam path to reduce the 6328-Å power to the level of the parametric fluorescence power. Care was taken to align the HeNe beam collinearly with the argon-ion laser beam so that the generated fluorescence power and HeNe beam were incident on the same area of the filters and photomultiplier surface. Measurements were then made at various acceptance angles. At each acceptance angle the background power was also determined by rotating the $LiIO_3$ crystal angle away from the phase-matching angle. The background power was typically 2% of the fluorescence power. Finally, the argon-ion pump power was remeasured to check that there was insignificant power drift during the run. The use of the balance measurement procedure ensured that the Eppley Thermopile and the photomultiplier were operating well within their linear response range. Thus we accurately compared the argon-ion laser and helium-neon laser powers and the parametric fluorescence and attenuated HeNe reference signal powers.

The results of the parametric fluorescence measurements are shown in Table I. For $LiIO_3$ the measured phase-matching angles agree very well with those calculated from the $LiIO_3$ indices of refraction.[20] The index of refraction values were also used to determine the dispersion constant $b$. Table I shows the measured values of $d_{31}$ and the number of independent measurements in parentheses. The final column gives the weighted average using standard statistical treatment of the data.[21] Table I also lists the results for the $LiNbO_3$ ($d_{31}$) coefficient measurements. In this case the dispersion constant was calculated using the congruent index of refraction data by Nelson and Mikulyak.[22]

The uncertainty in these measurements stems from the calibration of the neutral density filters. A typical 30-dB filter was calibrated to about 3% accuracy and since 80 dB of attenuation was required, the uncertainty amounts to about 10%. A small additional uncertainty arises from the power-ratio measurement, the determination of the dispersion constant, and from the phasematching angle.

The results of the measurements are compared to previous parametric fluorescence measurements in Fig. 2. The only accurate previous measurement of $d_{31}(LiIO_3)$ is by Campillo and Tang.[14] Their value of $d_{31} = (7.5 \pm 1.1) \times 10^{-12}$ m/V is in very good agreement with our best recommended value of $d_{31} = (7.31 \pm 0.62) \times 10^{-12}$ m/V determined by a

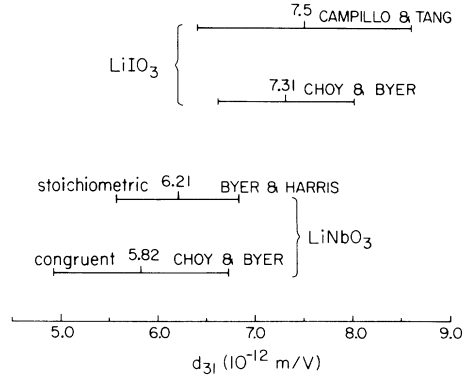


FIG. 2. Comparison of absolute values of $d_{31}(LiIO_3)$ and $d_{31}(LiNbO_3)$ determined by this measurement and by previous parametric fluorescence measurements.

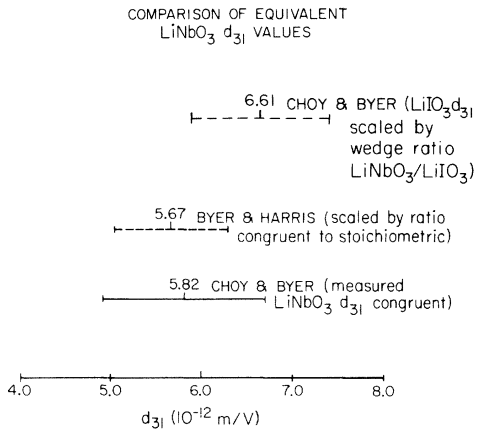


FIG. 3. Comparison of $d_{31}(LiNbO_3)$, this measurement, to $d_{31}(LiNbO_3)$ scaled by composition factor and comparison of $d_{31}(LiIO_3)$ to $d_{31}(LiNbO_3)$ scaled by wedge measurement ratio.

weighted average of the Miller's $\Delta$ of the 4880 and 5145 Å data.

For $LiNbO_3$ Byer and Harris[13] previously measured $d_{31} = (6.21 \pm 0.62) \times 10^{-12}$ m/V for stoichiometrically grown material. That measurement was an average of three independent determinations. Our present value of $d_{31} = (5.82 \pm 0.70) \times 10^{-12}$ m/V for congruently grown $LiNbO_3$ is somewhat lower than the earlier result. However, Miller *et al.*[23] have experimentally determined that the $d_{31}$ coefficient of $LiNbO_3$ is dependent upon crystal composition. Using their measured values, the ratio $d_{31}$ (congruent) to $d_{31}$ (stoichiometric) $= 0.913$. Thus the early measurement of $d_{31}$ by Byer and Harris should be reduced by this factor to compare with the present measurement. This comparison is shown in Fig. 3. The "adjusted" Byer-Harris value is $d_{31}$ (congruent) $= 5.67 \times 10^{-12}$ m/V which is in remarkably good agreement with the present value.

Figure 3 also shows the measured $d_{31}(LiIO_3)$ value scaled by ratio of the $LiNbO_3$ to $LiIO_3$ $d_{31}$ nonlinear coefficients as determined by wedge measurements at 1.318 $\mu$m to be discussed in Sec. III. The measured wedge ratio at 1.318 $\mu$m has been scaled through Miller's $\Delta$ to 4880 Å for this comparison. The result confirms that the parametric fluorescence method is indeed very accurate for the absolute determination of nonlinear coefficients. Of the four independent measurements of $d_{31}$ for $LiIO_3$ and $LiNbO_3$ all are well within the assigned error limits.

Because of the absence of compositional change in $LiIO_3$, its relatively large nonlinear coefficient, and the availability of quality crystals, the $d_{31}$ coefficient of $LiIO_3$ provides the optimum reference nonlinear coefficient. The accurate determination by parametric fluorescence of the $LiIO_3$ ($d_{31}$) coefficient provides the basis for comparative measurements using the wedge technique.

## III. WEDGE TECHNIQUE

### A. Theory

The two methods available for the intercomparison of nonlinear coefficients are the Maker fringe method[24,25] and the wedge technique.[26-28] The complications in data reduction introduced by the crystal rotation in the Maker fringe method make the simpler wedge technique preferable for nonlinear coefficient comparison measurements. A complete and thorough analysis of the wedge technique including the effects of absorption and finite beam width has been given by Chemla and Kupecek.[27] Boyd *et al.*[28] also have discussed the wedge technique from a more physical viewpoint and have arrived at results in agreement with Chemla and Kupecek. Here we summarize the principal results useful in reducing measurements made by the wedge technique.

For second-harmonic generation (SHG) the relation between the Fourier amplitude of the generated polarization and peak electric field is

$$P(\omega_2) = \epsilon_0 d_{\text{eff}} E^2(\omega_1), \tag{4}$$

where $\omega_1$ and $\omega_2$ are the fundamental and second-harmonic frequencies and $d_{\text{eff}}$ is the effective nonlinear coefficient. The nonlinear coefficient in mks units is related to the cgs value by $d_{\text{cgs}}$ (cm/statvolt) $= (c \times 10^{-4}/4\pi) = 2386\, d_{\text{mks}}$(m/V) where $c = 2.99793 \times 10^8$ m/sec.

The second-harmonic intensity at the output surface of a lossless crystal of length $l$ in the plane-wave approximation is given by

$$I_2 = (2\omega_1^2 d_{\text{eff}}^2 I_1^2 / n_1^2 n_2 \epsilon_0 c^3) l^2 \operatorname{sinc}^2 \varphi, \tag{5}$$

where $\omega_1$ is the fundamental frequency, $n_1$ and $n_2$ are the indices of refraction at the fundamental and second-harmonic frequencies, and $\operatorname{sinc}\varphi$ denotes the function $(1/\varphi)\sin\varphi$. The intensity is related to the electric field by

$$I = \tfrac{1}{2} n c \epsilon_0 |E|^2. \tag{6}$$

The phase factor $\varphi$ is defined by

$$\varphi = \tfrac{1}{2} \Delta k l = \pi l / 2 l_{\text{coh}} \tag{7}$$

and the coherence length is

$$l_{\text{coh}} = \lambda_1 / 4(n_1 - n_2). \tag{8}$$

Equation (5) must be generalized to include the effects of crystal loss and the finite width of the Gaussian laser beam. For the wedge measurement this is most easily done by using the results of Boyd *et al.*[28] If we let $K = 2\omega_1^2 d_{\text{eff}}^2 / \pi n_1^2 n_2 \epsilon_0 c^3$, then

the second-harmonic power at the output surface of the wedge for the lossless case and normal incidence is

$$I_2(x,y) = \pi K(2l_{\rm coh}/\pi)^2 I_1^2(x,y)\sin^2\varphi'. \quad (9)$$

The phase factor $\varphi'$ is a function of wedge geometry

$$\varphi' = \varphi + \tfrac{1}{2}\pi x(\tan\theta)/l_{\rm coh}, \quad (10)$$

where $\varphi$ is given by Eq. (7) and $x$ is the distance along the wedge with $\theta$ the wedge angle. If $L$ is the distance between SHG fringe minima, then

$$l_{\rm coh} = \tfrac{1}{2}L\tan\theta. \quad (11)$$

The second-harmonic power is found by integrating the intensity over the transverse dimensions

$$P_2 = \int_{-\infty}^{\infty} I_2(x,y)\,dx\,dy,$$

which gives

$$P_2 = (KP_1^2/w_1^2)l^2[S(F,\varphi)/\varphi^2], \quad (12)$$

where

$$S = \tfrac{1}{2}[1 - F\cos(\pi l/l_{\rm coh})]. \quad (13)$$

Here $F$ is the fringe visibility factor

$$F = \exp(-\tfrac{1}{16}\pi^2\eta^2) \quad (14)$$

with

$$\eta = w_1(\tan\theta)/l_{\rm coh}, \quad (15)$$

where $w_1$ is the Gaussian beam radius at the fundamental. Experimentally $F$ is determined from the fringe visibility since

$$F = (P_2^{\max} - P_2^{\min})/(P_2^{\max} + P_2^{\min}) \quad (16)$$

for small losses. For finite loss factors of $\alpha_1$ and $\alpha_2$ at the fundamental and second harmonic, Eq. (13) for the modulation factor generalizes to[27]

$$S = \tfrac{1}{2}e^{-(\alpha_1+\alpha_2/2)l}[\cosh(\alpha_1 - \tfrac{1}{2}\alpha_2)l - F\cos 2\varphi]. \quad (17)$$

Finally, we must relate the internal powers in the wedge given by Eq. (12) to the external powers actually measured. To do this we use the power transmission coefficient at a dielectric interface

$$T = 4n/(n+1)^2. \quad (18)$$

The observed SHG power at the detector is therefore

$$P_2 = T_1^2T_2\frac{KP_1^2l^2}{w_1^2}\frac{S(F,\varphi)}{\varphi^2} = \frac{4T_1^2T_2KP_1^2l_{\rm coh}^2S(F,\varphi)}{\pi^2w_1^2}. \quad (19)$$

The wedge comparison measurement is usually done without changing important parameters such as the laser power frequency or spot size. Thus the SHG power ratio between wedge $A$ and wedge $B$ is

$$\frac{P_{2A}}{P_{2B}} = \frac{n_{1B}^2n_{2B}T_{1A}^2T_{2A}d_A^2P_{1A}^2l_{{\rm coh}-A}^2S_A(F_A,\varphi)}{n_{1A}^2n_{2A}T_{1B}^2T_{2B}d_B^2P_{1B}^2l_{{\rm coh}-B}^2S_B(F_B,\varphi)}.$$

Substituting for $T$ from Eq. (18) and assuming $P_{1A} = P_{1B}$, the nonlinear coefficient ratio is

$$\frac{d_A}{d_B} = \left(\frac{P_A}{P_B}\right)^{1/2}\frac{(n_{1A}+1)^2(n_{2A}+1)}{(n_{1B}+1)^2(n_{2B}+1)} \times\frac{l_{{\rm coh}-B}}{l_{{\rm coh}-A}}\left(\frac{S_B(F_B,\varphi)}{S_A(F_A,\varphi)}\right)^{1/2}. \quad (20)$$

This equation was used to reduce the data and to determine the nonlinear coefficient ratios. In general Eq. (13) was used for $S(F,\varphi)$ except for GaAs and $AgGaSe_2$ where the loss was sufficient enough to warrant the use of Eq. (17).

### B. Experimental apparatus and measurement procedure

Figure 4 shows a schematic of the measurement apparatus. A Chromatix model 1000 acousto-optic $Q$-switched YAlG:Nd laser was the primary pump source. The laser operated at repetition rates between 10 and 20 Hz with peak-to-peak stability between 5 and 10%. The laser was operated at 1.318 $\mu$m and frequency doubled to generate 0.65 $\mu$m using an internal $LiIO_3$ angle phase-matched crystal. Peak output powers of a few kW were generated in the infrared. The laser was followed by a Corning 1-69 filter to eliminate 1.318 $\mu$m and then by a lens to properly focus the 0.659 $\mu$m radiation into a temperature tuned $LiNbO_3$ parametric oscillator. The parametric oscillator was tuned to 2.12 $\mu$m to provide a pump wavelength within the transparency range of both the visible and infrared crystals. The parametric oscillator was followed by a polarizer and filter to eliminate 0.659 $\mu$m radiation and the parametric oscillator signal wave at 0.956 $\mu$m.

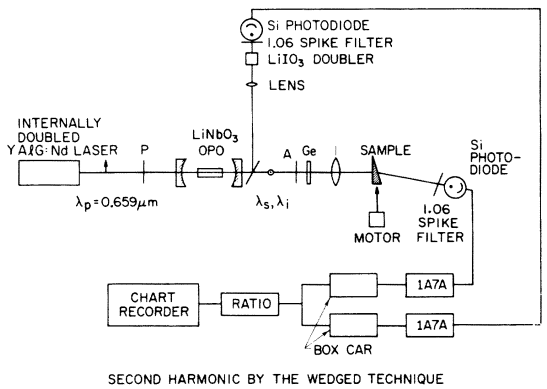


FIG. 4. Schematic of the experimental setup for the wedge technique measurements.

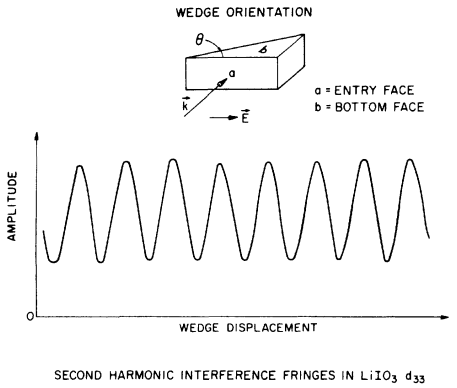


FIG. 5. Second-harmonic interference fringes in $d_{33}(LiIO_3)$ at 0.659 $\mu$m.

The 2.12 $\mu$m output of the parametric oscillator was focused with a 10 cm lens onto the wedge plane. Prior to the wedge, part of the beam was sent through a reference $LiIO_3$ crystal. The generated second harmonic then passed through a 1.06-$\mu$m interference filter and onto the reference silicon diode detector. The primary beam passed through the wedge sample, a similar 1.06-$\mu$m interference filter onto a matched silicon diode detector.

For these measurements the wedge was oriented to normal incidence by using the 0.695-$\mu$m visible beam, which propagated collinearly with the 2.12-$\mu$m beam, as an aid for wedge alignment. Following alignment to normal incidence, the wedge was adjusted to obtain the maximum signal by translation along the wedge and then by translation along the focused 2.12-$\mu$m beam. A vertically directed HeNe beam was used as a visual reference to help define the optimum wedge position within the 2-mm depth focal region. Once properly located the wedge was translated by a stepper motor driven micrometer stage.

The output of the matched silicon photodiodes was amplified by a pair of calibrated gain model 502 Tektronix preamplifiers, and then fed to a Molectron two channel dual gate differential boxcar integrator. The integrated signal channel output was then normalized to the reference channel in a ratio module and then recorded.

Careful attention was paid to the calibration and linearity of the electronics prior to a data run. A series of checks showed that the overall accuracy of the electronics was ±2% including reading error of the chart recorder. The calibrated gain of the Tektronix 502 preamplifiers was found to be significantly less than 2%. Thus gain adjustments

TABLE II. $d_{eff}$ and $l_{coh}$.

| Materials | $d_{eff}$ | $n_\omega$ | $n_{2\omega}$ | $l_{coh}$ Calc. | $l_{coh}$ Meas. |
|---|---|---|---|---|---|
| | | (a) at $\lambda = 2.12$ $\mu$m | | | |
| $LiIO_3$ | $d_{33}$ | 1.706 00 | 1.716 46[a] | 50.67 | 49.1 ±0.7 |
| $LiNbO_3$ | $d_{33}$ | 2.122 72 | 2.156 10[b] | 15.88 | 15.7 ±0.3 |
| GaP | $d_{36}$ | 3.035 0 | 3.106 5[d] | 7.41 | 7.5 ±0.2 |
| GaAs | $d_{36}$ | 3.346 5 | 3.479[e] | 4.00 | 3.8 ±0.15 |
| $AgGaSe_2$ | $d_{36}$ | 2.634 55 | 2.678 87[f] | 11.96 | 12.1 ±0.7 |
| CdSe | $d_{33}$ | 2.485 82 | 2.557 21[g] | 7.42 | 6.9 ±0.4 |
| | | (b) at $\lambda = 1.318$ $\mu$m | | | |
| $LiIO_3$ | $d_{31}\sin 20°$ | 1.850 63 | $n^e(20)$ = 1.858 83 [a] | 40.18 | 42.3 ±2.1 |
| $LiIO_3$ | $d_{33}$ | 1.712 55 | 1.732 67 [a] | 16.38 | 16.4 ±0.25 |
| $LiNbO_3$ | $d_{31}$ | 2.219 91 | 2.197 10[b] | 14.45 | 14.2 ±0.7 |
| $LiNbO_3$ | $d_{33}$ | 2.145 39 | 2.197 10[b] | 6.37 | 6.4 ±0.2 |
| KDP | $d_{36}$ | 1.486 07 | 1.466 16[c] | 16.55 | 15.8 ±1 |
| GaP | $d_{36}$ | 3.072 7 | 3.287 4[d] | 1.535 | 1.53 ±0.07 |

[a] R. L. Herbst (private communication). The $LiIO_3$ indices of refraction are given in Appendix A for reference.

[b] D. F. Nelson and R. M. Mikulyak, J. Appl. Phys. 45, 3688 (1974).

[c] F. Zernike, Jr., J. Opt. Soc. Am. 54, 1215 (1964).

[d] W. L. Bond, J. Appl. Phys. 36, 1674 (1965).

[e] D. T. F. Marple, J. Appl. Phys. 35, 1941 (1964).

[f] G. D. Boyd, H. M. Kasper, J. H. McFee, and F. G. Storz, IEEE J. Quant. Electron QE-8, 900 (1972). We have fitted a Sellmeir by combining the Boyd *et al.* data with our $AgGaSe_2$ mixing results.

[g] R. L. Herbst and R. L. Byer, Appl. Phys. Lett. 19, 527 (1971).

were made at the preamplifiers when required.

The measurements were taken in a sandwich pattern usually consisting of the reference wedge [$LiIO_3$ ($d_{33}$) or $LiNbO_3$ ($d_{33}$)], the sample wedge followed by the reference wedge. During this sequence, which usually took approximately 10 to 15 min including wedge orienting time, the critical parameters in the measurement such as laser power setting, repetition rate, filtering, and focusing were kept constant. In this way systematic effects were minimized. Figure 5 shows a sample of the data taken at 1.318-$\mu$m input. The signal amplitude limit was set by the burn density of the wedge samples at the power and spot size used.

Measurements at 1.318 $\mu$m were taken in a manner similar to those at 2.12 $\mu$m. The minor modifications in the setup included the direct use of the $Q$-switched YAlG:Nd laser source at 1.318 $\mu$m and the use of 0.659-$\mu$m interference filters to adequately filter against unwanted signals. The lack of silicon diode response at 1.318 $\mu$m aided in the spectral filtering. Increased laser power and increased diode sensitivity at 0.659 $\mu$m relative to that at 1.06 $\mu$m gave a significant improvement in signal-to-noise ratio for this set of measurements.

### C. Wedge measurement results

In presenting data of this type one is torn between the need for completeness and the requirement for brevity. We have chosen to present in tabular form the data essential to the interpretation of the measurement results.

Table II(a) lists the wedges, their effective nonlinear coefficients, indices of refraction, and calculated and measured coherence lengths for the 2.12-$\mu$m measurements. Table II(b) lists the same data for the wedges used for the 1.318-$\mu$m measurements. With the exception of GaAs, which is known to have a variable index of refraction and dispersion depending upon the sample and CdSe where the dispersion near the band gap is not accurately known, the agreement between measured and calculated coherence lengths is within 5%.

TABLE III. Wedge measurements at 2.12 $\mu$m.

| Crystal | $d_{\text{eff}}$ | $R=\frac{d_{\text{eff}}}{d_{33}\,(LiIO_3)}$ |
|---|---|---|
| (a) Relative to $LiIO_3$ ($d_{33}$) | | |
| $LiNbO_3$ | $d_{33}$ | 4.24 ±0.43 |
| GaP | $d_{36}$ | 12.1 ±1.1 |
| GaAs | $d_{36}$ | 25.5 ±1.0 |
| $AgGaSe_2$ | $d_{36}$ | 10.4 ±0.89 |
| CdSe | $d_{33}$ | 10.6 ±0.91 |
| Crystal | $d_{\text{eff}}$ | $R=\frac{d_{\text{eff}}}{d_{33}\,(LiNbO_3)}$ |
| (b) Relative to $LiNbO_3$ ($d_{33}$) | | |
| $LiIO_3$ | $d_{33}$ | 0.21 ±0.013 |
| GaAs | $d_{36}$ | 6.24 ±0.30 |
| $AgGaSe_2$ | $d_{36}$ | 2.28 ±0.21 |
| CdSe | $d_{33}$ | 2.01 ±0.16 |

The wedges ranged in size from 1 cm in length by 5 mm in height to greater than $1\times1$ cm$^2$. Wedge angles were cut to provide good fringe visibility but at the same time provide three or more fringes over the length of the wedge. The wedges were x-ray oriented to ±6 min of arc and polished to better than $\frac{1}{4}$ wave flatness in the visible. After fabrication, the wedge angles were measured by an autocollimator and by HeNe laser beam. The wedge angles used were: $LiIO_3$, (a) 10° 46′ 57″ ± 40″, (b) 10° 50′ 15″ ± 40″; $LiNbO_3$, 2° 25′ 31″ ± 40″; GaAs, (a) 1° 36′ 36″ ± 30″, (b) 1° 33′ 21″ ± 30″; GaP, 0° 52′ 27″ ± 10″; CdSe, 1° 18′ 58″ ± 50″; AgGaSe, 1° 46′ 59″ ± 50″. The optical quality of the wedges was excellent with the exception of $AgGaSe_2$, which gave reasonable fringes but showed some scattering of the incident beam.

If we denote the crystallographic axes by $x$, $y$, and $z$ being the optic axis, the wedges were orientated in the following manner. For $LiIO_3$ ($d_{33}$) the entry face is a $y$ face, the base face is an $x$ face with the incoming polarization along the $z$ axis. For $LiIO_3$ ($d_{31}$) the light propagates in the $x$, $y$ plane making a 45° angle to both the $x$ and $y$ axes. The normal of the base face makes an angle of 68° with the $z$ axis with the incident polarization being an ordinary ray. For $LiNbO_3$ ($d_{31}$) the light travels along the $x$ axis, the base face is a $z$ plane, and the incident polarization is ordinary. For $LiNbO_3$ ($d_{33}$) the propagation direction is the $x$ axis, the base face is a $y$ plane, and the incident polarization is extraordinary. For the $\bar{4}3$ m and $\bar{4}2$ m structure of KDP, GaP, GaAs, and $AgGaSe_2$, the propagation direction is a [110] axis. The base face is a $z$ plane and the incident polarization along the [$\bar{1}$10] axis. Finally for CdSe ($d_{33}$) light travels along the $x$ axis, the base face is a $z$ plane, and the incident polarization is along the $y$ axis.

In order to alleviate systematic measurement

TABLE IV. Wedge measurements at 1.318 $\mu$m relative to $LiIO_3$ ($d_{33}$).

| Crystal | $d_{\text{eff}}$ | $R=\frac{d_{\text{eff}}}{d_{33}(LiIO_3)}$ |
|---|---|---|
| $LiIO_3$ | $d_{31}$ | 1.01 ±0.06 |
| $LiNbO_3$ | $d_{31}$ | 0.87 ±0.057 |
| $LiNbO_3$ | $d_{33}$ | 4.71 ±0.30 |
| KDP | $d_{36}$ | 0.089 ±0.005 |
| GaP | $d_{36}$ | 12.20 ±0.71 |

TABLE V. Independent intercomparison wedge measurements.

| Coefficient ratio | λ | R |
|---|---|---|
| $d_{31}(LiNbO_3)/d_{31}(LiIO_3)$ | 1.318 μm | 0.869 ±0.095 |
| $d_{36}(GaP)/d_{33}(LiNbO_3)$ | 1.318 μm | 2.52 ±0.2 |
| $d_{36}(GaAs)/d_{33}(LiNbO_3)$ | 2.12 μm | 6.80 ±0.5 |

errors, we took two independent sets of measurements at 2.12 μm. One set was taken using $LiIO_3$ ($d_{33}$) as the standard and the other using $LiNbO_3$ ($d_{33}$) as the standard. In addition, the operator and setup was different in each case. Tables III(a) and III(b) display the measured nonlinear coefficient ratios at 2.12 μm. Estimated errors are also shown.

The measurements at 1.318 μm were taken with $LiIO_3$ ($d_{33}$) as the reference wedge. The data and results are given in Table IV. Finally, separate measurements were taken to intercompare $LiNbO_3$ $d_{33}$ and $d_{31}$ and $LiIO_3$ $d_{33}$ and $d_{31}$, and GaP and GaAs. These results are shown in Table V.

During the wedge measurements an analyzer was not used after the wedge since in many cases the generated second harmonic was polarized parallel to the input beam. In the case of the $LiNbO_3$ ($d_{31}$) coefficient the lack of an analyzer leads to an additional second-harmonic contribution due to the $d_{22}$ coefficient.[29] Correction for this contribution is discussed in Appendix B.

The wedge ratio results at 2.12 and 1.318 μm present an overdetermined set of measurements. It is therefore straightforward to check the accuracy of the measurements by looking for consistency ratios. In Table VI(a) we list consistency ratios taken at 1.318 μm. The measurements used, the table from which they were taken, and the measured ratios are listed. Agreement is seen to be excellent. Table VI(b) lists the consistency ratios at 2.12 μm. Here agreement is also very good but with slightly larger differences due to decreased signal to noise in the measurements.

Finally, based on the measurements presented in Tables III–V recommended ratios relative to $d_{31}(LiIO_3)$ are given in Table VII. The errors listed in Table VII were arrived at by statistical treatment of the wedge measurement data for the particular measurement wavelength. These relative nonlinear coefficient ratios are the principal results of the wedge measurements.

## IV. COMPARISON AND DISCUSSION OF RESULTS

### A. Recommended absolute susceptibilities at various wavelengths

The known dispersion of the second-order susceptibility with wavelength presents problems in establishing absolute values over an extended wavelength range. We have therefore scaled the susceptibility through Miller's[30] Δ which previously has been shown to be relatively constant even through strongly dispersive wavelength regions of

TABLE VI. Consistency ratios

| Ratio | Measurement table | Measured ratio | Comparison |
|---|---|---|---|
| | (a) At 1.318 μm | | |
| $d_{31}(LiIO_3)/d_{33}(LiIO_3)$ | IV | 1.01 | |
| $d_{31}(LiNbO_3)/d_{33}(LiIO_3)$ | IV | 0.879 | 1.01 |
| $d_{31}(LiNbO_3)/d_{31}(LiIO_3)$ | V | 0.869 | |
| $d_{33}(LiNbO_3)/d_{33}(LiIO_3)$ | IV | 4.71 | 5.34 |
| $d_{31}(LiNbO_3)/d_{33}(LiIO_3)$ | IV | 0.879 | |
| $d_{33}(LiNbO_3)/d_{33}(LiIO_3)$ | IV | 4.71 | |
| $d_{31}(LiNbO_3)/d_{31}(LiIO_3)$ | V | 0.869 | 5.35 |
| $d_{31}(LiIO_3)/d_{33}(LiIO_3)$ | IV | 1.01 | |
| | (b) At 2.12 μm | | |
| $d_{36}(GaAs)/d_{33}(LiNbO_3)$ | III(b) | 6.24 | |
| $d_{36}(GaAs)/d_{33}(LiNbO_3)$ | V | 6.80 | |
| $d_{36}(GaAs)/d_{33}(LiIO_3)$ | III(a) | 25.5 | 5.36 |
| $d_{33}(LiIO_3)/d_{33}(LiNbO_3)$ | III(b) | 0.21 | |
| $d_{33}(CdSe)/d_{33}(LiIO_3)$ | III(a) | 10.6 | |
| $d_{33}(CdSe)/d_{33}(LiNbO_3)$ | III(b) | 2.01 | 9.57 |
| $d_{33}(LiNbO)_3/d_{33}(LiIO_3)$ | III(b) | 4.76 | |
| $d_{33}(LiIO_3)/d_{33}(LiNbO_3)$ | III(b) | 0.21 | |
| $d_{36}(AgGaSe_2)/d_{33}(LiIO_3)$ | III(a) | 10.4 | 0.22 |
| $d_{36}(AgGaSe_2)/d_{33}(LiNbO_3)$ | III(b) | 2.28 | |

TABLE VII. Recommended ratios relative to $LiIO_3$ ($d_{31}$).

| Coefficient ratio | λ (μm) | Ratio |
|---|---|---|
| $d_{33}(LiIO_3)/d_{31}(LiIO_3)$ | 1.318 | 0.99 ±0.05 |
| $d_{31}(LiNbO_3)/d_{31}(LiIO_3)$ | 1.318 | 0.87 ±0.072 |
| $d_{33}(LiNbO_3)/d_{31}(LiIO_3)$ | 1.318 | 4.66 ±0.56 |
| | 2.12 | 4.53 ±0.43 |
| $d_{36}(KDP)/d_{31}(LiIO_3)$ | 1.318 | 0.088 ±0.01 |
| $d_{36}(GaP)/d_{31}(LiIO_3)$ | 1.318 | 12.0 ±1.2 |
| | 2.12 | 12.1 ±1.7 |
| $d_{36}(GaAs)/d_{31}(LiIO_3)$ | 2.12 | 26.9 ±2.1 |
| $d_{36}(AgGaSe_2)/d_{31}(LiIO)_3$ | 2.12 | 10.5 ±1.2 |
| $d_{33}(CdSe)/d_{31}(LiIO)_3$ | 2.12 | 10.2 ±1.2 |

a material.[31-33] Miller's Δ is related to the nonlinear tensor by

$$\Delta_{ijk} = d_{ijk}/\epsilon_0 \chi_{ii}(\omega_1)\chi_{jj}(\omega_2)\chi_{kk}(\omega_3), \quad (21)$$

where $\chi_{ii}(\omega_1)$, etc., are the linear susceptibilities in the crystallographic principal axes system. In scaling through Miller's Δ we have invoked Kleinman's[34] symmetry condition and used the principal values of the linear susceptibilities according to actual experimental conditions.

The best absolute value of Miller's Δ was determined by a weighted mean based on the parametric fluorescence measurements of $d_{31}(LiIO_3)$ at 4880 and 5145 Å. Table VIII lists the Miller's Δ values at 4880 and 5145 Å for $LiIO_3$ ($d_{31}$) and also lists the weighted mean value of $\Delta_{31} = (6.54 \pm 0.55) \times 10^{-2}$ m²/C. The indicated error comes directly from the measurement error of $d_{31}(LiIO_3)$ since the indices of refraction are known to a relatively high degree of accuracy for $LiIO_3$. Miller's Δ for $LiNbO_3$ is also listed in Table VIII.

Using the $LiIO_3$ Miller's Δ value obtained from the weighted mean, we then scaled back through the indices of refraction to determine a best nonlinear coefficient value at 4880 Å. This procedure gives for $d_{31}(LiIO_3)$ at 4880 Å a value of $d_{31} = (7.31 \pm 0.62) \times 10^{-12}$ m/V. This is the value displayed in Fig. 2 and is our best recommended value for $d_{31}(LiIO_3)$.

To establish a connection between the absolute parametric fluorescence measurements at 4880 Å and the wedge ratios relative to $d_{31}(LiIO_3)$ at 1.318 and 2.12 μm we assumed that Miller's Δ for $LiIO_3$ was constant. Using the $\Delta_{31}(LiIO_3)$ value given in Table VIII we then determined a nonlinear coefficient at 1.318 and 2.12 μm. These values are $d_{31}(LiIO_3) = 6.82 \times 10^{-12}$ and $6.43 \times 10^{-12}$ m/V. Table IX then lists the nonlinear coefficient values at 1.318 and 2.12 μm determined through the wedge ratios given in Table VII for the materials we have considered. We also list the indices of refraction and Miller's Δ for these materials. We have not listed the accuracy of the Miller's Δ values, but with the exception of GaAs and GaP, the error is determined by the wedge ratio and $LiIO_3$ Miller's Δ measurement error. The indices of refraction of GaAs and GaP are not now known accurately enough and need to be redetermined before a better value of Miller's Δ can be obtained.

Table X lists the recommended nonlinear coefficient values at various fundamental wavelengths of interest. These values are based on the $LiIO_3$ ($d_{31}$) parametric fluorescence measurement scaled through the wedge ratios using Miller's Δ as discussed above. Column five of Table X lists the method by which the particular nonlinear coefficient was determined. Here PF, MD, and W-$IO_3$ ($d_{31}$) refer to parametric fluorescence, Miller's Δ, and wedge measurement with respect to $d_{31}(LiIO_3)$. In the case of $LiNbO_3$ ($d_{31}$), $LiNbO_3$ ($d_{33}$), and GaP ($d_{36}$) the coefficients values were overdetermined. In these cases a mean Miller's Δ was used to determine the nonlinear coefficient value. For example, $\Delta_{31}(LiNbO_3)$ has a value of $1.00 \times 10^{-2}$ m²/C by parametric fluorescence and $1.13 \times 10^{-2}$ m²/C determined through the wedge ratio relative to $d_{31}(LiIO_3)$. Thus the best recommended $d_{31}(LiNbO_3)$ value given in Table X is slightly greater than the value determined from the parametric fluorescence result.

### B. Comparison with previous measurements

In Sec. II we discussed the comparison of our parametric fluorescence determined $LiIO_3$ ($d_{31}$)

TABLE VIII. Experimentally determined Miller's Δ's by parametric fluorescence.

| Materials | λ (μm) | $n(\omega_1)$ | $n(\omega_2)$ | $n(\omega_3)$ | $d_{31}$ ($10^{-12}$ m/V) | $\Delta_{31}$ ($10^{-2}$ m²/C) | |
|---|---|---|---|---|---|---|---|
| $LiIO_3$ | 0.6328+2.1326 →0.4880 | 1.88074 | 1.84085 | 1.75591 | 7.215 | 6.46 | $\Delta_{31}$ (weighted mean) = 6.54 |
| | 0.6328+2.7521 →0.5145 | 1.88074 | 1.83409 | 1.75053 | 7.330 | 6.69 | |
| $LiNbO_3$ | 0.6328+2.1326 →0.4880 | 2.28678 | 2.19275 | 2.25610 | 5.823 | | 1.00 |

TABLE IX. Experimentally determined Miller's Δ's by wedged technique relative to $d_{31}(LiIO_3)$.

| Materials | $\lambda_{fundamental}(\mu m)$ | $n_\omega$ | $n_{2\omega}$ | $d_{ij}$ ($10^{-12}$ m/V) | $\Delta_{ij}$ ($10^{-2}$ m$^2$/C) |
|---|---|---|---|---|---|
| $LiIO_3$ | 1.318 | 1.712 55 | 1.732 67 [a] | $d_{33}=6.75$ | 10.2 |
| $LiNbO_3$ | 1.318 | 2.219 91 | 2.197 10 [b] | $d_{31}=5.93$ | 1.13 |
| | 1.318 | 2.145 39 | 2.197 10 | $d_{33}=31.8$ | 7.23 |
| | 2.12 | 2.122 72 | 2.156 10 | $d_{33}=29.1$ | 7.34 |
| KDP | 1.318 | 1.486 07 | 1.466 16 [c] | $d_{36}=0.599$ | 4.04 |
| GaP | 1.318 | 3.072 72 | 3.287 37 [d] | $d_{36}=81.7$ | 1.32 |
| | 2.12 | 3.035 02 | 3.106 54 | $d_{36}=77.5$ | 1.50 |
| GaAs | 2.12 | 3.346 52 | 3.479 [e] | $d_{36}=173.$ | 1.70 |
| $AgGaSe_2$ | 2.12 | 2.634 55 | 2.678 87 [f] | $d_{36}=67.7$ | 3.51 |
| CdSe | 2.12 | 2.485 82 | 2.557 21 [g] | $d_{33}=65.4$ | 4.97 |

[a] R. L. Herbst (private communication). The $LiIO_3$ indices of refraction are given in Appendix A for reference.
[b] D. F. Nelson and R. M. Mikulyak, J. Appl. Phys. 45, 3688 (1974).
[c] F. Zernike, Jr., J. Opt. Soc. Am. 54, 1215 (1964).
[d] W. L. Bond, J. Appl. Phys. 36, 1674 (1965).
[e] D. T. F. Marple, J. Appl. Phys. 35, 1941 (1964).
[f] G. D. Boyd, H. M. Kasper, J. H. McFee, and F. G. Storz, IEEE J. Quant. Electron QE-8, 900 (1972).
[g] R. L. Herbst and R. L. Byer, Appl. Phys. Lett. 19, 527 (1971).

and $LiNbO_3$ ($d_{31}$) nonlinear coefficient values with previous absolute determinations. In this section we are primarily concerned with comparing the recommended values given in Table X with previous relative nonlinear coefficient measurements. This is because, with the exception of CdSe and pyrargyrite, previous absolute measurements were made by SHG and are relatively inaccurate.

We first consider our recommended value for $d_{36}(KDP)=0.63\times10^{-12}$ m/V at 1.064 μm. Francois[5] and later Bjorkholm and Siegman[6] independently measured $d_{36}(ADP)$ at 0.6328 μm and found $d_{36}=(0.57\pm0.07)\times10^{-12}$ m/V and $d_{36}=(0.58\pm0.09)\times10^{-12}$ m/V. These values were determined by SHG of a 0.6328-μm helium-neon laser and used the same Epply thermopile for the absolute power measurement. Scaling Francois's value to 1.06 μm gives $d_{36}(ADP)=0.50\times10^{-12}$ m/V. Finally, scaling to KDP through the ratio $d_{36}(ADP)/d_{36}(KDP)$ of $1.21\pm0.05$ determined by Jerphagnon and Kurtz[35] gives $0.41\times10^{-12}$ m/V for the Francois value. This value is low compared to our value of $0.63\times10^{-12}$ m/V. However, Bechmann and Kurtz[36] suggest a higher value for $d_{36}(KDP)$ of $0.63\pm12\times10^{-12}$ m/V, which is in agreement with our value. Bechmann and Kurtz, however, did not give the wavelength of their value or how it was determined.

Nath and Hussuhl's[37] first measurement of $d_{31}(LiIO_3)$ relative to $d_{31}(LiNbO_3)$ is about a factor of 2 high. Relative measurements by Nash *et al.*[38] of $d_{31}(LiIO_3)$ to $d_{36}(KDP)$ of $11\pm1.5$ agree very well with our ratio of $11.3\pm3.1$. Nash *et al.* also determined the ratio $d_{33}(LiIO_3)$ to $d_{31}(LiIO_3)$ of $0.8\pm0.25$, which agrees with our value of $0.99\pm0.05$. Jerphagnon[2] using the Maker fringe method, carefully measured $LiIO_3$ nonlinear coefficients. His ratio of $d_{31}(LiIO_3)$ to $d_{36}(KDP)$, of $11.9\pm1$, is in close agreement with our value. Jerphagnon's ratio of $d_{33}(LiIO_3)$ to $d_{31}(LiIO_3)$ of $1.04\pm0.08$ is also in close agreement with our value of 0.99. Taken together, Nash *et al.*, Jerphagnon, and our ratio values show remarkably good agreement. A recent measurement by Pearson *et al.*[39] of $d_{31}(LiIO_3)$ to $d_{36}(KDP)$ at ruby wavelength of $11.2\pm1.2$ agrees within error to our value of $12.1\pm3.3$. All of these measurements support our value of $7.11\times10^{-12}$ m/V for $d_{31}(LiIO_3)$ at 1.06 μm, which is significantly larger than the value of $(5.53\pm0.3)\times10^{-12}$ m/V recommended by Levine and Bethea.[4]

$LiNbO_3$ presents a special problem because of the compositional dependence of the $d_{31}$ coefficient.[23] Early measurements by Boyd *et al.*[29] of $d_{31}(LiNbO_3)$ to $d_{36}(KDP)$ of $11.9\pm1.7$ agree well with our ratio of $9.4\pm2.9$ if account is taken of the stoichiometric-to-congruent $d_{31}$ ratio of 1.09. Thus the Boyd *et al.* value reduces to 10.8 which is well within error limits compared to our value. Boyd *et al.* also determined the ratio $d_{33}(LiNbO_3)$ to $d_{36}(KDP)$ of $107\pm20$ compared to our value of 54.5. Kleinman and Miller[40] measured the ratio $d_{33}(LiNbO_3)$ to $d_{31}(LiNbO_3)$ of $6.0\pm1$ at 1.15 μm. Our value for the same ratio of coefficients is $5.78\pm1.9$. However, Kleinman and Miller's value must be increased by the stoichiometric-to-con-

TABLE X. Recommended absolute values at various wavelengths. MD, Miller's Δ; PF, parametric fluorescence; W, wedge; $*\lambda_p = 0.4880 \rightarrow 0.6328 + 2.133$ μm.

| Material | $d_{ij}$ | λ (μm) | $10^{-12}$ m/V | Method |
|---|---|---|---|---|
| $LiIO_3$ | $d_{31}$ | 2.12 | 6.43 | MD |
| | | 1.318 | 6.82 | PF + MD |
| | | 1.06 | 7.11 | MD |
| | | 0.6943 | 8.41 | MD |
| | | $*\lambda_p = 0.4880$ | 7.31 ±0.62 | PF |
| | $d_{33}$ | 2.12 | 6.41 | MD |
| | | 1.318 | 6.75 ±0.95 | $W$-$IO_3$($d_{31}$) |
| | | 1.06 | 7.02 | MD |
| $LiNbO_3$ | $d_{31}$ | 1.318 | 5.54 ±0.61 | PF + MD $W$-$IO_3$($d_{31}$) |
| | | 1.15 | 5.77 | MD |
| | | 1.06 | 5.95 | MD |
| | | $*\lambda_p = 0.4880$ | 6.18 ±0.68 | PF + $W$-$IO_3$ ($d_{31}$) |
| | $d_{33}$ | 2.12 | 29.1 ±5.2 | $W$-$IO_3$($d_{31}$) |
| | | 1.318 | 31.8 ±6.4 | $W$-$IO_3$($d_{31}$) |
| | | 1.15 | 33.4 | MD |
| | | 1.06 | 34.4 | MD |
| KDP | $d_{36}$ | 1.318 | 0.599 ±0.11 | $W$-$IO_3$($d_{31}$) |
| | | 1.15 | 0.619 | MD |
| | | 1.06 | 0.630 | MD |
| | | 0.6328 | 0.712 | MD |
| GaP | $d_{36}$ | 10.6 | 58.1 | MD |
| | | 3.39 | 65.5 | MD |
| | | 2.12 | 77.5 ±17 | $W$-$IO_3$($d_{31}$) |
| | | 1.318 | 81.7 ±15 | $W$-$IO_3$($d_{31}$) |
| | | 1.06 | 99.7 | MD |
| GaAs | $d_{36}$ | 10.6 | 151 | MD |
| | | 2.12 | 173 ±28 | $W$-$IO_3$($d_{31}$) |
| $AgGaSe_2$ | $d_{36}$ | 10.6 | 57.7 | MD |
| | | 2.12 | 67.7 ±13 | $W$-$IO_3$($d_{31}$) |
| CdSe | $d_{33}$ | 10.6 | 55.3 | MD |
| | | 2.12 | 65.4 ±13 | $W$-$IO_3$($d_{31}$) |

gruent ratio of 1.09 to give 6.54, which is still well within error limits. More recently, Bjorkholm[41] measured the ratio $d_{31}(LiNbO_3)$ to $d_{36}$(KDP) and obtained 10.9 ± 1.7 at 1.15 μm. Our ratio of 9.3 ± 2.9 is in good agreement with Bjorkholm's value. Finally, Levine and Bethea[4] recommend for $d_{31}(LiNbO_3)$ the value $(5.45 \pm 0.3) \times 10^{-12}$ m/V compared to our value of $(5.95 \pm 0.71) \times 10^{-12}$ m/V at 1.06 μm.

The $d_{31}$ coefficient of CdSe has been measured absolutely in a mixing experiment by Herbst and Byer.[8] In the experiment a single-mode 10.6-μm $CO_2$ laser was mixed with 1.833 μm from a YAlG:Nd laser to generate 2.22 μm. Herbst[42] gives for $d_{31}$(CdSe) a value of $(22 \pm 3) \times 10^{-12}$ m/V. If we take our value of $\Delta_{33}$(CdSe) and scale it to the above wavelengths, we find $d_{33}(CdSe) = 59.02 \times 10^{-12}$ m/V. Using the known geometric ratio[43,44] $d_{33}/d_{31} = 2$ we find $d_{31}(CdSe) = 29.5 \times 10^{-12}$ m/V, which is in good agreement with Herbst's absolute value.

Boyd *et al.*[45] have determined the ratio $d_{31}$(CdSe) to $d_{36}$(GaAs) at 10.6 μm and found 0.2 ± 0.02. Our ratio of $d_{33}$(CdSe) to $d_{36}$(GaAs) at 10.6 μm is 0.37 which gives a $d_{31}$(CdSe) to $d_{36}$(GaAs) ratio of 0.18 ±0.06 which is again in good agreement with the Boyd *et al.* value. This comparison shows that scaling through Miller's Δ from 2.12 to 10.6 μm is valid to within experimental error.

$AgGaSe_2$ has been studied by three groups because of its useful phasematching properties for infrared generation by mixing and SHG. Boyd *et al.*[46] measured a ratio $d_{36}(AgGaSe_2)$ to $d_{36}$(GaAs) at 10.6 μm of 0.368 ± 0.04. This is in good agreement with our ratio of 0.38 ± 0.1. Kildal and Mikkelsen[47] measured an absolute value of $d_{36}(AgGaSe_2)$ at 10.6 μm by SHG and obtained $d_{36} = (32.4 \pm 0.5) \times 10^{-12}$ m/V. Byer *et al.*[48] also measured $d_{36}(AgGaSe_3)$ by SHG of a 10.6-μm laser and obtained $d_{36} = (37.4 \pm 6) \times 10^{-12}$ m/V. These values are somewhat low compared to our recommended value of $(57.7 \pm 11) \times 10^{-12}$ m/V. Since the absolute measurements were obtained by SHG of a $CO_2$ laser using relatively lower-quality material than that presently available, the lower absolute values are not unexpected. In the same paper, Byer *et al.*[48] also measured $d_{36}$(AgGaSe) to $d_{36}$(GaAs) and obtained 0.33 ± 0.08 and 0.32 ± 0.06. Again these relative measurements agree well with our value of 0.38 ± 0.1. This discussion of the $AgGaSe_2$ coefficient value shows that absolute SHG measurements in the infrared are difficult to make with potential large systematic errors due to laser mode control, focusing, and material quality variations.

An absolute value for $d_{36}$(GaAs) has been determined by McFee *et al.*[49] by a measurement relative to $Ag_3SbS_3$, which has been absolutely determined by phasematched SHG of 10.6 μm. The value given in $d_{36}(GaAs) = (134 \pm 42) \times 10^{-12}$ m/V, which is in quite good agreement with our value of $d_{36} = (151 \pm 24) \times 10^{-12}$ m/V. In contrast, Levine and Bethea's best fit $d_{36}$(GaAs) value is $(90 \pm 4.5) \times 10^{-12}$ m/V, which is considerably below the above values.

Using the wedge technique Wynne and Bloembergen[26] have measured the ratio $d_{36}$(GaAs) to $d_{36}$(InAs) at 10.6 μm and find 0.45. Using Wynne and Bloembergen's absolute value of $d_{14}$(InAs) determined by SHG at 10.6 μm of $(419 \pm 200) \times 10^{-12}$ m/V, their value for $d_{36}$(GaAs) is $(188 \pm 94) \times 10^{-12}$ m/V, which is on the high side of both McFee *et al.* and our value. Wynne and Bloembergen also measured the ratio of $d_{36}$(GaP) to $d_{36}$(GaAs) through InAs at 10.6 μm and find 0.58. We find a ratio of

$0.38 \pm 0.13$ at 10.6 $\mu$m through Miller's $\Delta$ scaling of our 2.12-$\mu$m wedge measurements.

An absolute measurement of $d_{36}$(GaAs) was also made by Johnston and Kaminow[11] using Raman scattering at 1.06 $\mu$m. Their value of $(140 \pm 10) \times 10^{-12}$ m/V compares reasonably well with our value of $(173 \pm 28) \times 10^{-12}$ m/V at 2.12 $\mu$m. These values are in good agreement considering the material variations from sample to sample and the inaccuracies in the measured linear index of refraction of GaAs.

GaP nonlinear coefficient has been measured relative to KDP by Miller[30] who found $d_{36}(\mathrm{GaP})/d_{36}(\mathrm{KDP}) = 175 \pm 30$ at 1.06 $\mu$m. Our value is 158 $\pm$ 63 which is in good agreement. More recently Levine and Bethea measured GaP relative to $SiO_2$ and obtained $d_{36}(\mathrm{GaP})/d_{11}(\mathrm{SiO_2}) = 185 \pm 19$ at 1.318 $\mu$m. Using Jerphagnon's ratio of $d_{31}(\mathrm{LiIO_3})/d_{11}(\mathrm{SiO_2}) = 15.5 \pm 0.8$ at 1.06 $\mu$m and our recommended ratio of $d_{36}(\mathrm{GaP})/d_{31}(\mathrm{LiIO}) = 14.0 \pm 2.8$ at 1.06 $\mu$m we find a $d_{36}$(GaP) to $d_{11}(\mathrm{SiO_2})$ ratio of $217 \pm 54$ at 1.06 $\mu$m instead of 1.318 $\mu$m. This measurement of the GaP nonlinear coefficient by Levine and Bethea is in good agreement with our value. Furthermore, their $d_{36}$(GaAs) to $d_{36}$(GaP) ratio at 10.6 $\mu$m of 2.16 agrees with our value of $2.59 \pm 0.9$.

The use of GaAs and GaP as standard crystals in the infrared presents difficulties due to material variations and the lack of precise values of the indices of refraction. When better index of refraction data become available our ratio values presented in Table VII of GaAs and GaP relative to $LiIO_3$ can be used to determine a Miller's $\Delta$ value and to scale to other infrared wavelengths.

## V. CONCLUSION

In establishing our recommended nonlinear coefficient values listed in Table X we have taken care to scale to various wavelengths through the relatively dispersionless Miller's $\Delta$. Previously, nonlinear coefficients were directly compared at various wavelengths which has led to significant errors especially in the infrared where, in general, the second-order susceptibility is an order of magnitude larger than in the visible and dispersion is even more important. Our relative measurements by the wedge technique at 2.12 and 1.318 $\mu$m agree well with previous results over the wavelength range from the visible to 10.6 $\mu$m in the infrared. The good agreement lends further support to Miller's $\Delta$ scaling and the theoretical predictions by Bell[31] and others[33] that Miller's $\Delta$ is constant even in relatively high dispersion regions of a crystal's transparency range. However, a note of caution must be made regarding Miller's $\Delta$ scaling of GaAs and GaP to infrared wavelengths that approach the reststrahlen band. Faust and Henry[50] have measured the nonlinear coefficient of GaP through this region and have determined that due to interference[51] the nonlinear coefficient does not follow variations in the linear susceptibility.

The linear susceptibility used in scaling through Miller's $\Delta$ is well known for most visible and near infrared transparent crystals. The two notable exceptions are GaAs and GaP where a better determination of the index of refraction must be made.

In general, our relative nonlinear coefficient measurements using the wedge technique agree very well with previous relative measurements over a wide wavelength range. Our measurement accuracy is about the best that can be done without serious consideration to laser stabilization and automatic data processing.

Our absolute determination of $d_{31}(\mathrm{LiIO_3})$ and $d_{31}(\mathrm{LiNbO_3})$ by parametric fluorescence is in excellent agreement with previous parametric fluorescence determinations as described in Sec. IV B. When scaled through Miller's $\Delta$ and the wedge ratios, the absolute values recommended in Table X agree rather well with previous determinations as in the case of CdSe by mixing. However, absolute SHG measurements, such as for $AgGaSe_2$, show a larger disagreement as described previously.

With these measurements we have, for the first time, simultaneously compared the nonlinear susceptibilities of visible and infrared crystals. Using the parametric fluorescence method we have accurately determined the absolute suceptibility of $LiIO_3$ and have thus established an absolute reference for a nonlinear susceptibility scale that extends over both the visible and infrared spectral ranges.

## ACKNOWLEDGMENTS

We wish to acknowledge the assistance of Dr. S. K. Kurtz for providing the GaP wedge samples and for helpful discussions. We also want to acknowledge Dr. D. S. Chemla, Dr. J. Jerphagnon, and Dr. R. L. Herbst for their helpful comments. This work was supported by ARO and ERDA through LASL.

## APPENDIX A: $LiIO_3$ INDICES OF REFRACTION

The $LiIO_3$ indices of refraction have been measured by Herbst[20] using the minimum dispersion prism method over a wavelength range from 0.5461 to 5 $\mu$m. Table XI lists the measured indices and wavelengths. Using these values

TABLE XI. Measured refractive indices for $LiIO_3$.

| $\lambda$ ($\mu$m) | $n_0$ | $n_e$ |
|---|---|---|
| 0.5461 | 1.8942 | 1.7450 |
| 0.5790 | 1.8888 | 1.7407 |
| 0.6328 | 1.8815 | 1.7351 |
| 1.0139 | 1.8578 | 1.7172 |
| 1.0642 | 1.8517 | 1.7168 |
| 1.1287 | 1.8548 | 1.7151 |
| 1.3673 | 1.8504 | 1.7118 |
| 1.5295 | 1.8478 | 1.7100 |
| 2.0 | 1.8420 | 1.7064 |
| 2.5 | 1.8378 | 1.7037 |
| 3.0 | 1.8319 | 1.7001 |
| 3.5 | 1.8266 | 1.6971 |
| 4.0 | 1.8140 | 1.6897 |
| 5.0 | 1.7940 | 1.6783 |

Herbst computed a best fit Sellmeier equation for the ordinary and extraordinary indices of refraction of the form

$$n^2 = A + \frac{B}{1 - C/\lambda^2} + \frac{D}{1 - E/\lambda^2}, \tag{A1}$$

where $\lambda$ is in $\mu$m with the constants (see Table XII).

## APPENDIX B: CONTRIBUTION TO $LiNbO_3$ ($d_{31}$) WEDGE RATIOS

For a fundamental input wave polarized along the $y$ axis of $LiNbO_3$, both $\mathcal{P}_z$ and $\mathcal{P}_y$ second-harmonic polarization components are generated. Substituting these into Maxwell's equations we have, after integrating over a length $l$,

$$E_{2y} = K d_{22} l_{22} E_{1y}^2 \sin(\pi l/2l_{22}) e^{i\pi l/2l_{22}}, \tag{B1}$$

$$E_{2z} = K d_{31} l_{31} E_{1y}^2 \sin(\pi l/2l_{31}) e^{i\pi l/2l_{31}}, \tag{B2}$$

where the subscripts 1 and 2 denote the fundamental and harmonic fields, respectively, $l_{22} = \lambda/4(n_2^0 - n_1^0)$ and $l_{31} = \lambda/4(n_2^e - n_1^0)$ and $K$ is a constant. The total second-harmonic intensity is then given by the superposition of the ordinary and extraordinary harmonic beams. As these harmonic waves are orthogonally polarized, the interference cross term vanishes and the resultant output harmonic power is given by

$$|E_{2\omega}|^2 = |E_{2y}|^2 + |E_{2z}|^2$$

$$= K^2 E_{1y}^4 \left[ d_{22}^2 l_{22}^2 \sin^2\left(\frac{\pi l}{2l_{22}}\right) + d_{31}^2 l_{31}^2 \sin^2\left(\frac{\pi l}{2l_{31}}\right)\right]. \tag{B3}$$

The total external power due to both $d_{22}$ and $d_{31}$ contributions is given by

$$P(d_{31} + d_{22}) = \left(\frac{d_{31} l_{31}}{n_2^e + 1}\right)^2 \times \left[\sin^2\left(\frac{\pi l}{2l_{31}}\right) + \left(\frac{d_{22} l_{22}}{d_{31} l_{31}}\right)^2 \times \left(\frac{n_2^e + 1}{n_2^0 + 1}\right)^2 \sin^2\left(\frac{\pi l}{2l_{22}}\right)\right]$$

$$= P_{\max}(d_{31})\left[\sin^2\left(\frac{\pi l}{2l_{31}}\right) + \sim 4\%\right], \tag{B4}$$

where explicit power transmittance factors at the wedge surface have been included, and the knowledge of the $d_{22}/d_{31}$ ratio of 0.53 (Ref. 29) and the magnitude of the coherence lengths have been used. The coherence lengths are $l_{22} = 5.49$ $\mu$m and $l_{31} = 14.4$ $\mu$m. From the above values we find that the $d_{22}$ contribution results in a 4% amplitude modulation on the interference fringes. We have absorbed this factor into our error analysis.

TABLE XII. Values of the constants $A$–$E$ for $n_0$ and $n_e$.

| | $n_0$ | $n_e$ |
|---|---|---|
| $A$ | 2.03132 | 1.830 86 |
| $B$ | 1.376 23 | 1.088 07 |
| $C$ | $3.508\,32 \times 10^{-2}$ | $3.138\,10 \times 10^{-2}$ |
| $D$ | 1.067 45 | $5.545\,82 \times 10^{-1}$ |
| $E$ | $1.6900 \times 10^{+2}$ | $1.5876 \times 10^{2}$ |


*Now employed by Philips Laboratories, New York.

[1] J. Jerphagnon and S. K. Kurtz, Phys. Rev. B 1, 1739 (1970).

[2] J. Jerphagnon, Appl. Phys. Lett. 16, 298 (1970).

[3] D. S. Chemla, P. J. Kupecek, and C. A. Schwartz, Opt. Commun. 7, 225 (1973).

[4] B. F. Levine and C. G. Bethea, Appl. Phys. Lett. 20, 272 (1972).

[5] G. E. Francois, Phys. Rev. 143, 597 (1966).

[6] J. E. Bjorkholm and A. E. Siegman, Phys. Rev. 154, 851 (1967).

[7] J. F. Ward, Phys. Rev. 143, 569 (1966).

[8] R. L. Herbst and R. L. Byer, Appl. Phys. Lett. 19, 527 (1971).

[9] J. Ducuing and N. Bloembergen, Phys. Rev. 133, A1493 (1964).

[10] G. D. Boyd and D. A. Kleinman, J. Appl. Phys. 39, 3597 (1968).

[11] W. D. Johnston, Jr. and I. P. Kaminow, Phys. Rev. 188, 1209 (1969).

[12] W. D. Johnston, Jr. Phys. Rev. B 1, 3494 (1970).

[13] R. L. Byer and S. E. Harris, Phys. Rev. 168, 1064

(1968).
[14]A. J. Campillo and C. L. Tang, Appl. Phys. Lett. 16, 242 (1970).
[15]S. E. Harris, M. K. Oshman, and R. L. Byer, Phys. Rev. Lett. 18, 732 (1967).
[16]D. Magde and H. Mahr, Phys. Rev. Lett. 18, 905 (1967).
[17]T. G. Giallorenzi and C. L. Tang, Phys. Rev. 166, 225 (1968).
[18]D. A. Kleinman, Phys. Rev. 128, 1761 (1968).
[19]R. L. Byer, Ph.D. dissertation (Stanford University, 1968) (unpublished).
[20]R. L. Herbst (private communication). The $LiIO_3$ indices of refraction are given in Appendix A for reference.
[21]P. R. Bevington, *Data Reduction and Error Analyzer for Physical Sciences* (McGraw-Hill, New York, 1969).
[22]D. F. Nelson and R. M. Mikulyak, J. Appl. Phys. 45, 3688 (1974).
[23]R. C. Miller, W. A. Nordland, and P. M. Bridenbaugh, J. Appl. Phys. 42, 4145 (1971).
[24]P. D. Maker, R. W. Terhune, M. Nisenhoff, and C. M. Savage, Phys. Rev. Lett. 8, 21 (1962).
[25]J. Jerphagnon and S. K. Kurtz, J. Appl. Phys. 41, 1667 (1970).
[26]J. J. Wynne and N. Bloembergen, Phys. Rev. 188, 1211 (1969).
[27]D. Chemla and P. Kupecek, Rev. Phys. Appl. 6, 31 (1971).
[28]G. D. Boyd, H. Kaspar, and J. H. McFee, IEEE J. Quant. Electron QE-7, 563 (1971).
[29]G. D. Boyd, R. C. Miller, K. Nassau, W . L. Bond, and A. Savage, Appl. Phys. Lett. 5, 234 (1964).
[30]R. C. Miller, Appl. Phys. Lett. 5, 17 (1964).
[31]M. I. Bell, Phys. Rev. B 6, 516 (1972).
[32]H. Lotem and Y. Yacoby, Phys. Rev. B (to be published).
[33]D. Bethune, A. J. Schmidt, and Y. R. Shen, Phys. Rev. B 11, 3867 (1975).
[34]D. A. Kleinman, Phys. Rev. 126, 1977 (1962).
[35]J. Jerphagnon and S. K. Kurtz, Phys. Rev. B 1, 1739 (1970).
[36]R. Beckman and S. K. Kurtz, *Landolt-Borstein Numerical Data and Functional Relationships*, edited by K. H. Hellwege and A. M. Hellwege (Springer-Verleg, Berlin, 1969), Group III, Vol. 2.
[37]G. Nath and S. Haussuhl, Appl. Phys. Lett. 14, 154 (1969).
[38]F. R. Nash, J. G. Bergman, G. P. Boyd, and E. H. Turner, J. Appl. Phys. 40, 5201 (1969).
[39]J. E. Pearson, G. A. Evans, and A. Yariv, Opt. Commun. 4, 366 (1972).
[40]D. A. Kleinman and R. C. Miller, Phys. Rev. 148, 302 (1966).
[41]J. E. Bjorkholm, IEEE J. Quant. Elect. QE-4, 970 (1968); QE-5, 260 (1969).
[42]R. L. Herbst, Ph.D. dissertation (Stanford University, 1972 (unpublished).
[43]J. Jerphagnon, Phys. Rev. B 2, 1091 (1970).
[44]F. N. H. Robinson, Phys. Lett. A 26, 435 (1968).
[45]G. D. Boyd, E. Buehler, and F. G. Storz, Appl. Phys. Lett. 18, 301 (1971).
[46]G. D. Boyd, H. Kasper, J. H. McFee, and F. G. Storz, IEEE J. Quant. Elect. QE-8, 900 (1972).
[47]H. Kildal and J. C. Mikkelsen, Opt. Commun. 9, 315 (1973).
[48]R. L. Byer, M. M. Choy, R. L. Herbst, D. S. Chemla, and R. S. Feigelson, Appl. Phys. Lett. 24, 65 (1974).
[49]J. H. McFee, G. D. Boyd, and P. H. Schmidt, Appl. Phys. Lett. 17, 57 (1970).
[50]W. L. Faust and C. H. Henry, Phys. Rev. Lett. 17, 1265 (1966).
[51]C. Flytzanis, Phys. Rev. Lett. 23, 1336 (1969).